ORIGINAL SCIENTIFIC PAPER OPEN ACCESS

Analytical and numerical analysis of the modified 2D arc-star-shaped structure with negative Poisson's ratio

Vladimir Sinđelić[1*], Aleksandar Nikolić[1], Nebojša Bogojević[1], Snežana Ćirić Kostić[1], Giangiacomo Minak[2]

[1] University of Kragujevac, Faculty of Mechanical and Civil Engineering in Kraljevo, Kraljevo, Serbia

[2] Alma Mater Studiorum University of Bologna, Department of Industrial Engineering, Bologna, Italy

ARTICLE INFO

[*] **Correspondence:** sindjelic.v@mfkv.kg.ac.rs

DOI: 10.5937/engtoday2400004S

UDC: 621(497.11) **ISSN:** 2812-9474

Article history: Received 10 November 2023; Revised 19 January 2024; Accepted 24 January 2024

ABSTRACT

The Poisson's ratio represents one of the very important characteristics of mechanical metamaterials. Thanks to additive manufacturing, it is now much simpler to create structures for the study of Poisson's ratio. Particularly, for research purposes, re-entrant structures are of interest as they can exhibit negative values of Poisson's ratio. Due to their capabilities, such structures find extensive applications across various industries. The modified arc-star-shaped (m2D-AS) has been studied analytically and numerically, and the negative Poisson's ratio (NPR) and Young's modulus has been examined for different geometric parameters of the structure.

KEYWORDS

Mechanical metamaterial, Auxetic material, Negative Poisson's ratio (NPR), Arc-star-shaped structure, Young's modulus, Re-entrant structure, Finite element method (FEM), 3D design

1. INTRODUCTION

Mechanical metamaterials are artificially manufactured materials created to optimize the mass of a structure while retaining or improving specific mechanical properties of that structure. One of the new properties that can be imparted to mechanical metamaterials is their ability to exhibit a negative Poisson's ratio (NPR in the further). Unlike conventional structures, structures with NPR can contract when subjected to pressure loads, enabling them to possess efficient energy absorption characteristics, Figure 1. In the literature, structures with NPR are represented by two terms: "Re-entrant" and "Auxetic" [1]. Thanks to their capabilities, these structures find a wide range of applications in fields such as mechanical engineering, civil engineering, biomedicine, space industry, automotive industry, aerospace, sports equipment, etc.

A very popular structure with an NPR is the re-entrant honeycomb [2], which contracts in only one direction. However, in recent years, structures have been designed with re-entrant features in both directions. Structures of this shape are called star-shaped structures. Na Xu at all studied the influence of NPR and Young's modulus on three similar designs based on a star-shaped structure [3]. In their study, Xiang at all investigated the relationship between NPR and negative thermal expansion (NTE) in a designed structure based on a star-shaped structure [4]. The energy absorption in a star-shaped structure with different types of bonding in metamaterial was theoretically, numerically and experimentally studied, in [5].

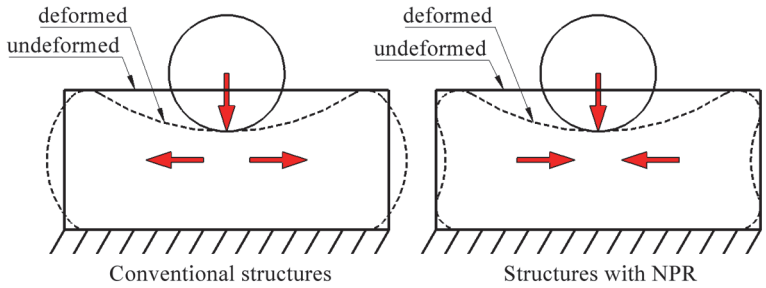

Figure 1: The difference between conventional structures and structures with NPR

A study from 2022 demonstrated the elastic mechanical properties of a novel 2D NPR structure obtained through the combination of a Re-entrant hexagon and star-shaped structure [6].In [7], the alteration of the geometry of the star-shaped structure led to an improvement in the mechanical properties of the structure. Zhang et all [8] designed a new structure inspired by the star-shaped structure, which they named the butterfly-shaped structure, to achieve higher stiffness while retaining the structure's ability to exhibit NPR. Zheng et all [9] investigated analytically, numerically, and experimentally the Poisson's ratio of the new structure, named the 2D arc-star-shaped structure (2D-AS in the further). In parallel with the structure developed in this paper, the authors also created another structure published in the paper [10].

This paper represents a continuation of the research in [11]. The structure presented in this paper has a simpler geometry, necessary for the development of an analytical model, compared to the structure presented in paper [10]. This fact gives us the possibility to obtain explicit expressions for displacements in the horizontal and vertical directions. An analytical model of the modified 2D arc-star-shaped structure (m2D-AS in the further) was developed using the energy method, and the analytical results were validated through finite element method (FEM in the further).

2. MODIFIED 2D ARC-STAR-SHAPED STRUCTURE

2.1. The design of the m2D-AS structure

The m2D-AS structure model is based on the 2D-AS structure model shown in Figure 2(a). The m2D-AS structure is designed by replacing the horizontal and vertical rods with a circular arc at the midpoint of the length AB, as shown in Figure 2(b). In addition to the geometric parameters that define 2D-AS, such as the length L, the height h, the depth d, the thickness t, the arc radius r, the arc angle θ, the length coefficients along the horizontal and vertical direction a and b and the total length in horizontal and vertical direction L_x and L_y [9], [11], the m2D-AS also has the arc radius R that replace the horizontal and vertical rods in the 2D-AS, shown in Figure 2(c).

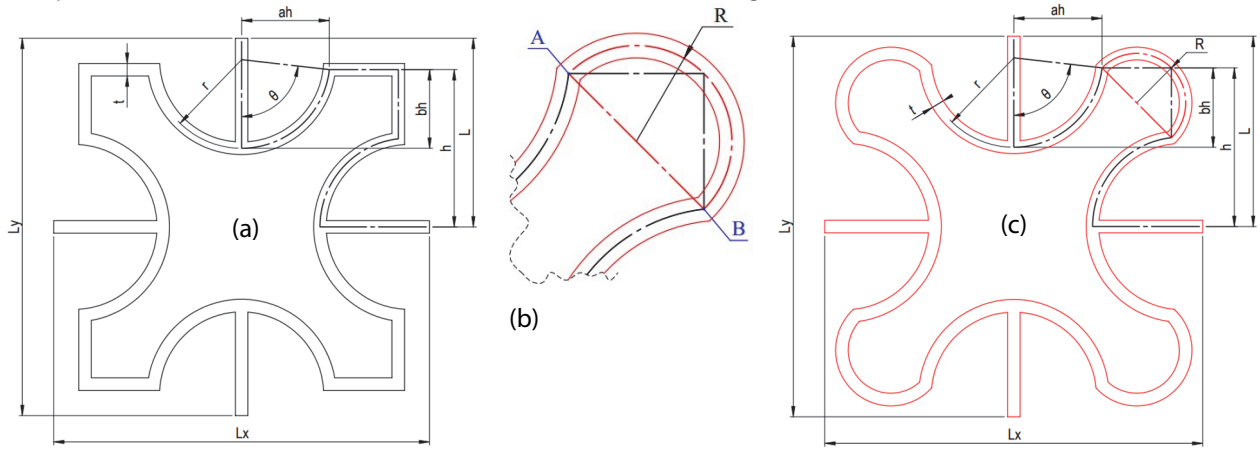

Figure 2: (a) The geometric parameters of 2D-AS [9], [11]; (b) Modification of a 2D-AS; (c) The geometric parameters of m2D-AS [11]

The length coefficients a and b are within the limits $0<a<1$ and $0<b<1$ [9], [11]. The relationship between geometric parameters a, b, h and θ, r, R is represented by the following expressions [9], [11]:

$$\theta = 2\arctan\frac{bh}{ah} \tag{1}$$

$$r = \frac{ah}{\sin\theta} \tag{2}$$

$$R = \frac{\sqrt{2}\cdot(h-ah)}{2} \tag{3}$$

According to the geometric parameters shown in Figure 1(c), an expression for the relative density of the m2D-AS has been derived [11]:

$$\rho_r = \frac{4t}{l_x l_y}\left(r\pi\frac{\theta}{90} + R\pi + l - h + bh\right) \tag{4}$$

2.2. Analytical model of the m2D-AS

The analytical model begins with the consideration of a single cell of the m2D-AS from an infinitely large structure, which is subject to axial loading in the vertical direction σ_y, as shown in Figure 3.

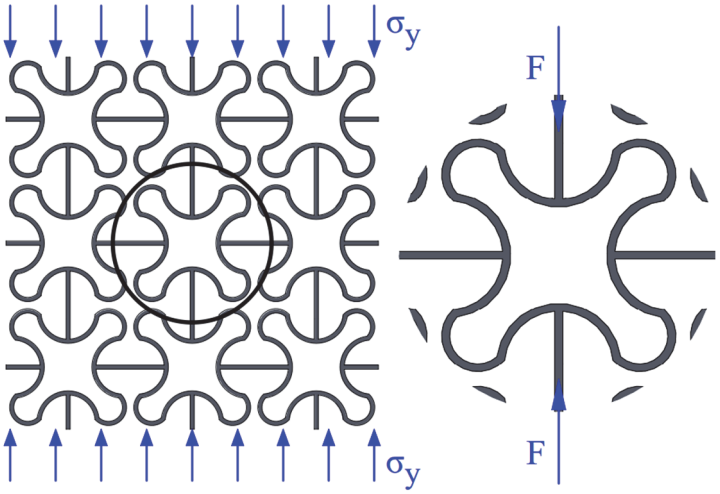

Figure 3: Periodic of modified 2D-AS lattice structure with a single cell under axial loading

For the analytical study of the Poisson's ratio and Young's modulus effects on the m2D-AS the energy method is used, and take into account the following assumptions:

1) The deformations are small and they belong to the elastic area,
2) The thickness of m2D-AS is much smaller compared to the length,
3) The structure is subjected only to bending deformations without the influence of stretching and shearing,
4) The joint of the m2D-AS are rigid.

Due to the symmetry of the structure, an analysis is performed on half of the m2D-AS under the action of the vertical force *F*. Then, this half is divided into two quarters, left and right, as shown in Figure 4. The mutual influence of the left and right quarters one on the other is described by the internal forces Y_O and Y_O' and moments M_O and M_O', which have the same magnitude but opposite directions.

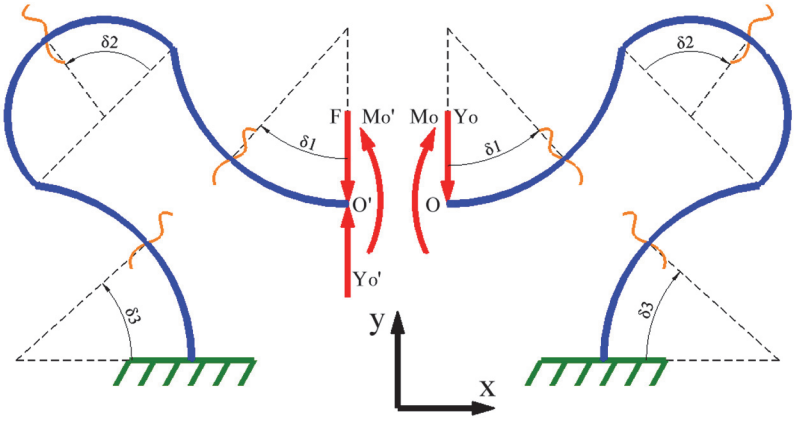

Figure 4: Dividing one half of the modified 2D-AS into quarters

The values of force Y_O and moment M_O under the action of the vertical force *F* are determined using the energy method, as expressed by the following equations:

$$\frac{\partial U}{\partial Y_O}+\frac{\partial U}{\partial Y_O'}=\frac{1}{EI}\left\{\int_0^{\theta}M_1\frac{\partial M_1}{\partial Y_O}rd\delta_1+\int_0^{\pi}M_2\frac{\partial M_2}{\partial Y_O}Rd\delta_2+\int_0^{\theta}M_3\frac{\partial M_3}{\partial Y_O}rd\delta_3\right\}+$$
$$+\frac{1}{EI}\left\{\int_0^{\theta}M_1'\frac{\partial M_1'}{\partial Y_O}rd\delta_1+\int_0^{\pi}M_2'\frac{\partial M_2'}{\partial Y_O}Rd\delta_2+\int_0^{\theta}M_3'\frac{\partial M_3'}{\partial Y_O}rd\delta_3\right\}=0 \tag{5}$$

$$\frac{\partial U}{\partial M_O}+\frac{\partial U}{\partial M_O'}=\frac{1}{EI}\left\{\int_0^{\theta}M_1\frac{\partial M_1}{\partial M_O}rd\delta_1+\int_0^{\pi}M_2\frac{\partial M_2}{\partial M_O}Rd\delta_2+\int_0^{\theta}M_3\frac{\partial M_3}{\partial M_O}rd\delta_3\right\}+$$
$$+\frac{1}{EI}\left\{\int_0^{\theta}M_1'\frac{\partial M_1'}{\partial M_O}rd\delta_1+\int_0^{\pi}M_2'\frac{\partial M_2'}{\partial M_O}Rd\delta_2+\int_0^{\theta}M_3'\frac{\partial M_3'}{\partial M_O}rd\delta_3\right\}=0 \tag{6}$$

where E is Young's modulus, I cross-section moment of inertia, M_1, M_2, M_3 and M_1', M_2', M_3' represent bending moments into the introduced fields for the right and left sides respectively. By solving equations (5) and (6), expressions for the support reactions at point O are derived:

$$Y_O=\frac{F}{2} \tag{7}$$

$$M_O=\frac{F}{4\pi R+8r\theta}\left(2r^2+2\sqrt{2}R^2+\sqrt{2}\pi R^2+2\sqrt{2}rR\theta+2r^2(-1+\theta)\cos\theta+2r\left(\pi R+r(-1+\theta)\right)\sin\theta\right) \tag{8}$$

$$\overline{M_O}=\frac{1}{4\pi R+8r\theta}\left(2r^2+2\sqrt{2}R^2+\sqrt{2}\pi R^2+2\sqrt{2}rR\theta+2r^2(-1+\theta)\cos\theta+2r\left(\pi R+r(-1+\theta)\right)\sin\theta\right) \tag{9}$$

where $\overline{M_O}$ is the unit moment. To determine horizontal and vertical displacements, a fictitious force $X_O=0$ is introduced at point O, as shown in Figure 5.

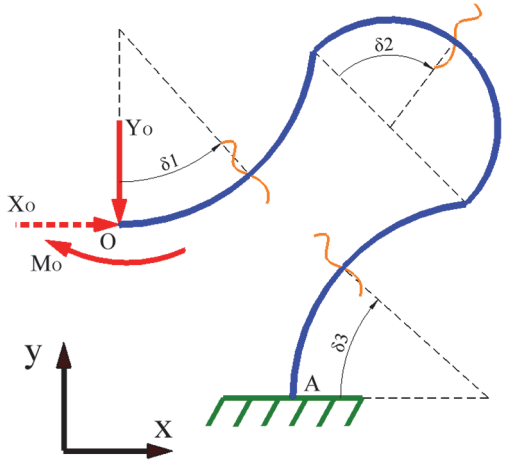

Figure 5: Displacement point O in the horizontal and vertical direction within a quarter of the m2D-AS

Using the energy method, the horizontal Δ_{xx} displacement of point O and vertical Δ_{yx} displacement of point A are determined as follows:

$$\Delta_{xx}=\frac{1}{EI}\left(\int_0^{\theta}M_1\cdot\frac{\partial M_1}{\partial X_O}rd\delta_1+\int_0^{\pi}M_2\cdot\frac{\partial M_2}{\partial X_O}Rd\delta_2+\int_0^{\theta}M_3\cdot\frac{\partial M_3}{\partial X_O}rd\delta_3\right) \tag{10}$$

$$\Delta_{yx}=\frac{1}{EI}\left(\int_0^{\theta}M_1\cdot\frac{\partial M_1}{\partial Y_O}rd\delta_1+\int_0^{\pi}M_2\cdot\frac{\partial M_2}{\partial Y_O}Rd\delta_2+\int_0^{\theta}M_3\cdot\frac{\partial M_3}{\partial Y_O}rd\delta_3\right) \tag{11}$$

From equations (10) and (11), we obtain:

$$\Delta_{xx}=\frac{F}{8E_sI}\begin{pmatrix}-2\pi R^3+2\sqrt{2}R^2\cdot\left(2\overline{M_O}(-2+\pi)+(2+\pi)r-(2+\pi)r\cos\theta-(-2+\pi)r\sin\theta\right)\\+r^2\left(r+2\left(-8\overline{M_O}+r\right)\theta+3r\cos2\theta+4\left(4\overline{M_O}+r(-1+\theta)\right)\sin\theta-2r\cos\theta(2-2\theta+\sin\theta)\right)\\-2rR\left(2\sqrt{2}r(-\theta+\sin\theta)-4\pi\sin\left(\frac{\theta}{2}\right)^2\left(-2\overline{M_O}+r\sin\theta\right)\right)\end{pmatrix} \tag{12}$$

$$\Delta_{yx} = \frac{F}{2E_s I}\begin{pmatrix} -2\overline{M_O}r^2 - (2+\pi)\left(\sqrt{2}\overline{M_O} - R\right)R^2 + 2rR\left(-\sqrt{2}\overline{M_O} + R\right)\theta + r^3(-1+2\theta) + r^3\cos 2\theta + \\ r\sin\theta\left(-2\overline{M_O}(\pi R + r(-1+\theta)) + \sqrt{2}R\left((2+\pi)R + 2r(-1+\theta)\right) + \pi rR\sin\theta\right) + \\ 2r^2\cos\theta\left(\overline{M_O} - \overline{M_O}\theta + \sqrt{2}R\theta + r(-1+\theta)\sin\theta\right) \end{pmatrix} \quad (13)$$

The expression for Poisson's ratio v and Young's modulus E_y can be written as [9], [11]:

$$\nu = -\frac{\varepsilon_x}{\varepsilon_y} = -\frac{\Delta_{xx}}{\Delta_{yx}} \cdot \frac{l_y}{l_x} \quad (14)$$

$$E_y = \frac{\sigma_y}{\varepsilon_y} = \frac{F}{4\Delta_{yx}} \cdot \frac{l_y}{l_x \cdot d} \quad (15)$$

2.2.1. Numerical example

Two sets of parameters were applied to determine the Poisson's ratio and Young's modulus. In the first set, the parameter *ah* varies from *8* to *22 mm* with a step of *1 mm*, while *bh=12.5 mm* is held constant. In the second set, *bh* varies from *8* to *22 mm* with a step of *1 mm*, while *ah* is held constant. The other parameters are fixed and have the following values *L=30 mm*, *h=25 mm*, *t=2 mm,* and *d=3 mm*. The results are presented in Table 1 and Table 2.

Table 1: The values of relative density, the Poisson's ratio, and Young's modulus for various values of the parameter *ah*

ah	**8**	**10**	**12**	**14**	**16**	**18**	**20**	**22**
$\boldsymbol{\rho_r}$	0.201	0.195	0.189	0.185	0.181	0.177	0.174	0.171
v	-0.035	-0.145	-0.257	-0.365	-0.461	-0.537	-0.587	-0.604
$\boldsymbol{E_y}$	0.226	0.259	0.292	0.327	0.362	0.398	0.435	0.471

Table 2: The values of relative density, the Poisson's ratio, and Young's modulus for various values of the parameter *bh*

bh	**8**	**10**	**12**	**14**	**16**	**18**	**20**	**22**
$\boldsymbol{\rho_r}$	0.160	0.172	0.185	0.198	0.212	0.227	0.242	0.258
v	-0.054	-0.149	-0.256	-0.372	-0.492	-0.609	-0.714	-0.802
$\boldsymbol{E_y}$	0.321	0.314	0.304	0.291	0.275	0.256	0.234	0.210

The influence of geometric parameters on the m2D-AS for relative density and Poisson's ratio is shown in Figure 6 and Figure 7 respectively.

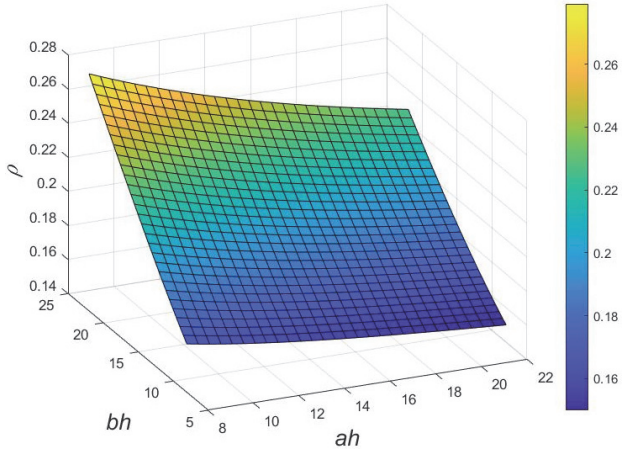

Figure 6: Effects of the parameter *ah* and *bh* on relative density ρ_r

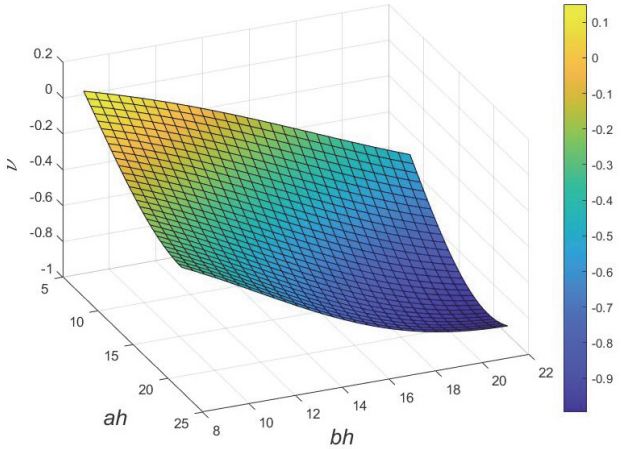

Figure 7: Effects of the parameter *ah* and *bh* on NPR

2.3. Numerical model of the m2D-AS

A numerical model for studying the Poisson's ratio and the Young's modulus of m2D-AS was created using the finite element method (FEM) in ANSYS. The material has the following characteristics: Young's modulus *E=1500 MPa*, density ρ*=0.92 g/cm*^{3}, and Poisson's ratio of material v_m*=0.4*. The type of finite elements used is *Hex20* and *Wed15*, with an element size of *1 mm*.

The numerical simulation was conducted in two sets as in section 2.2.1. The values of parameter *ah* range from *10* to *20 mm* with a *2 mm* increment and the values of parameter *bh* range from *10* to *18 mm* with a *2 mm* increment. In the m2D-AS, vertical displacement along the vertical beam in the y-axis direction was applied, and they amount to *3 mm*, and the results were measured along the horizontal beam in the x-axis direction, as shown in Figure 8(a)-(d). The results obtained with FEM are presented in Table 3 and Table 4.

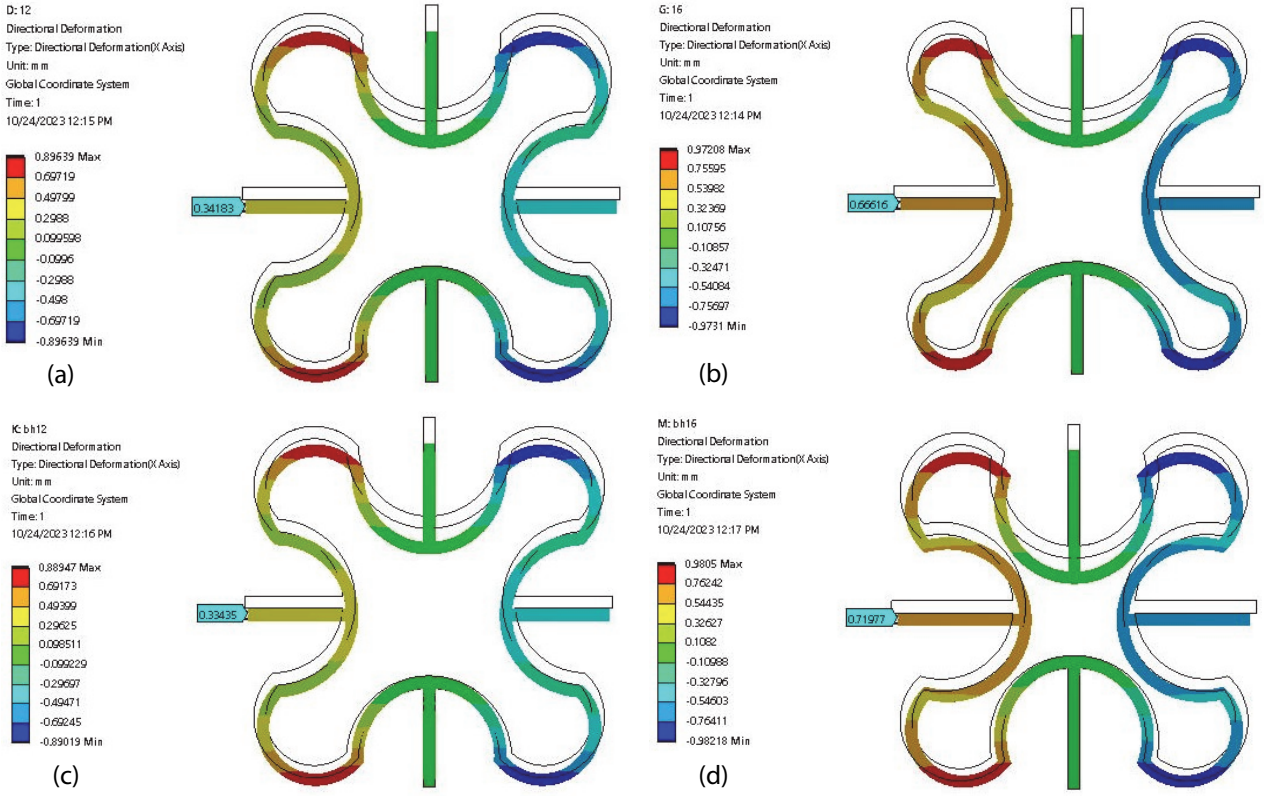

Figure 8: Horizontal displacement of m2D-AS for: (a) *ah=12 mm*, (b) *ah=16 mm*, (c) *bh=12 mm*, (d) *bh=16 mm*

Table 3: The values of the Poisson's ratio and Young's modulus obtained by FEM for various values of the parameter *ah*

ah	**8**	**10**	**12**	**14**	**16**	**18**	**20**
v	-0.001	-0.112	-0.228	-0.341	-0.444	-0.532	-0.598
E_y	0.207	0.236	0.266	0.298	0.33	0.363	0.396

Table 4: The values of the Poisson's ratio and Young's modulus obtained by FEM for various values of the parameter *bh*

bh	**8**	**10**	**12**	**14**	**16**	**18**
v	-0.054	-0.083	-0.223	-0.358	-0.480	-0.580
E_y	0.293	0.286	0.277	0.265	0.251	0.234

In Figure 9(a)-(d), comparative results for Poisson's ratio and Young's modulus obtained using the analytical method and the FEM, are shown.

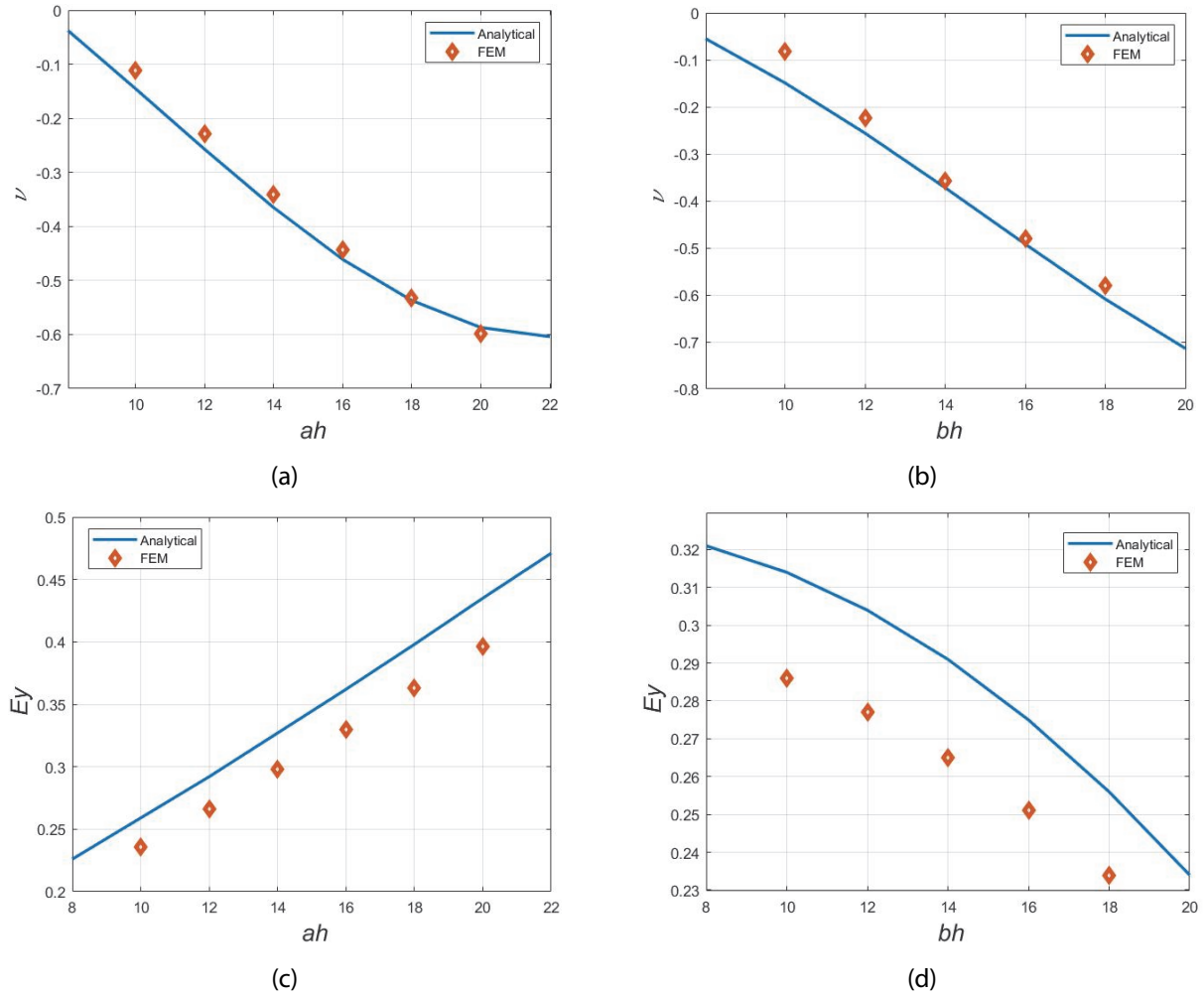

Figure 9: Analytical vs. FEM results (a) The comparison of *NPR* analytical and FEM for parameter *ah*, (b) The comparison of *NPR* analytical and FEM for parameter *bh*, (c) The comparison of E_y analytical and FEM for parameter *ah*, (d) The comparison of E_y analytical and FEM for parameter *bh*

3. CONCLUSION

In this paper, an analytical model for calculating NPR and Young's modulus for the structure presented in the paper [13] has been developed. The analytical model was developed based on the assumption that the cell is exposed only to bending, and the influence of stretching and shearing was not taken into account. As can be seen in the results shown in Figure 9(a) and 9(b), there is a very good agreement between the values of the FEM model and the analytical model. In the calculation of Young's modulus, significant deviations between the FEM model and the analytical model are shown in Figures 9(c) and 9(d). The absence of stretching and shearing in the analytical model can be considered as the cause of such discrepancies. In future work, it is essential to consider stretching and shearing when developing the analytical model. Additionally, exploring different types of connections and structures of similar shapes in 3D space should be investigated.

ACKNOWLEDGEMENTS

This research was supported under grant no. 451-03-47/2023-01/200108 by the Ministry of Education, Science and Technological Development of the Republic of Serbia. This support is gratefully acknowledged.

REFERENCES

[1] T.-C. Lim, "Mechanics of Metamaterials with Negative Parameters", Springer, Singapore (Singapore), https://doi.org/10.1007/978-981-15-6446-8, (2020)

[2] I. G. Masters and K. E. Evans, "Models for the elastic deformation of honeycombs", Composite Structures, Vol. 35(4) pp. 403–422, https://doi.org/10.1016/S0263-8223(96)00054-2, (1996)

[3] N. Xu, H. T. Liu, M. R. An, and L. Wang, "Novel 2D star-shaped honeycombs with enhanced effective Young's modulus and negative Poisson's ratio", Extreme Mechanics Letters, Vol. 43, p. 101164, https://doi.org/10.1016/j.eml.2020.101164, (2021)

[4] X. Li, L. Gao, W. Zhou, Y. Wang, and Y. Lu, "Novel 2D metamaterials with negative Poisson's ratio and negative thermal expansion", Extreme Mechanics Letters, Vol. 30, p. 100498, https://doi.org/10.1016/j.eml.2019.100498, (2019)

[5] X. Li, Z. Li, Z. Guo, Z. Mo, and J. Li, "A novel star-shaped honeycomb with enhanced energy absorption", Composite Structures, Vol. 309, p. 116716, https://doi.org/10.1016/j.compstruct.2023.116716, (2023)

[6] Y. T. Jin, Y. H. Qie, N. N. Li, and N. W. Li, "Study on elastic mechanical properties of novel 2D negative Poisson's ratio structure: Re-entrant hexagon nested with star-shaped structure", Composite Structures, Vol. 301, p. 116065, https://doi.org/10.1016/j.compstruct.2022.116065, (2022)

[7] W. Liu, H. Li, J. Zhang, X. Gong, Y. Wang, and X. Ge, "Tensile and shear properties of star-shaped cellular lattice structure", Mechanics of Advanced Materials and Structures, Vol. 28(24), pp. 2605–2617, https://doi.org/10.1080/15376494.2020.1747669, (2021)

[8] Z. W. Zhang, R. L. Tian, X. L. Zhang, F. Y. Wei, and X. W. Yang, "A novel butterfly-shaped auxetic structure with negative Poisson's ratio and enhanced stiffness", Journal of Materials Science, Vol. 56(25), pp. 14139–14156, https://doi.org/10.1007/s10853-021-06141-4, (2021)

[9] Z. Y. Zhang, J. Li, H. T. Liu, and Y. Bin Wang, "Novel 2D arc-star-shaped structure with tunable Poisson's ratio and its 3D configurations", Materials Today Communications, Vol. 30, p. 103016, https://doi.org/10.1016/j.mtcomm.2021.103016, (2022)

[10] V. Sinđelić, A. Nikolić, G. Minak, N. Bogojević, and S. Ćirić Kostić, "An improved 2D arc-star-shaped structure with negative Poisson's ratio: In-plane analysis", Materials Today Communications, Vol. 37, p. 107593, https://doi.org/10.1016/j.mtcomm.2023.107593, (2023)

[11] V. Sinđelić, A. Nikolić, N. Bogojević, O. Erić Cekić, and S. Ćirić Kostić, "Modified 2D arc-star-shaped structure with negative Poisson's ratio", Proceedings of XI International Conference "Heavy Machinery HM 2023", Vrnjačka Banja (Serbia), p. E.21-E.26, (2023)